Electronic Supplementary Material (ESI) for Polymer Chemistry.

High-Performance Polyamides with Engineered Disorder

Supporting Information

Nicolas Candau,[1,2,‡] Sylvain Galland,[1,2,‡] Julien Cretenoud,[1] Sandor Balog,[3] Véronique Michaud,[2]

Jean-Marc Chenal,[4] Olivier Lame,[4] Christopher J.G. Plummer,[1] Holger Frauenrath[1,]*

[1] Laboratory of Macromolecular and Organic Materials (LMOM), Institute of Materials (IMX), Ecole Polytechnique Fédérale de Lausanne (EPFL), Station 12, 1015 Lausanne, Switzerland

[2] Laboratory for Processing of Advanced Composites (LPAC), Institute of Materials (IMX), Ecole Polytechnique Fédérale de Lausanne (EPFL), Station 12, 1015 Lausanne, Switzerland

[3] Adolphe Merkle Institute, University of Fribourg, Switzerland

[4] University of Lyon, INSA de Lyon, MATEIS, CNRS, UMR 5510, 69621 Villeurbanne, France

† These authors have equally contributed to the paper

Glossary

Thermomechanical properties

ε_b: strain at break (%)

E: Young Modulus (MPa)

σ_y: Yield stress (MPa)

T_g: Glass transition (°C)

T_m: melting temperature (°C)

Materials

PA66: poly(hexamethylene adipamide)

PA610: poly(hexamethylene sebacoamide)

PA12: poly(laurolactam)

PA6TI: poly(hexamethylene terephthalamide-co isophthalamide)

PA6T: poly(hexamethylene terephthalamide)

PA6TI-PA66: random copolyamides of PA6TI and PA66

PA6TI-PA610: random copolyamides of PA6TI and PA610

PA6TI/PA12: blends of PA6TI and PA12

T6T: terephthalamide-hexamethylene-terephthalamide sequence

I units: isophthaloyl units

T units: terephthaloyl units

Supplementary Figures S1–S8

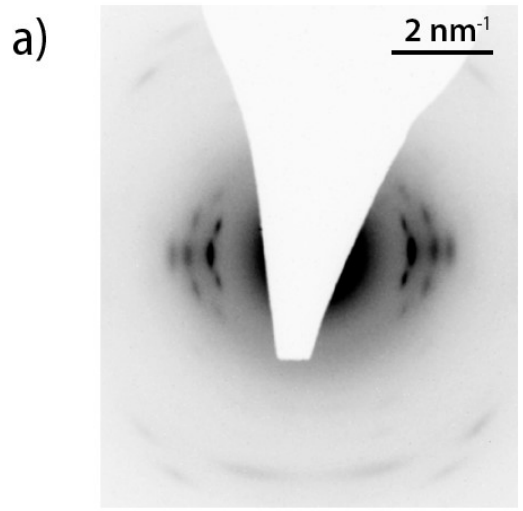

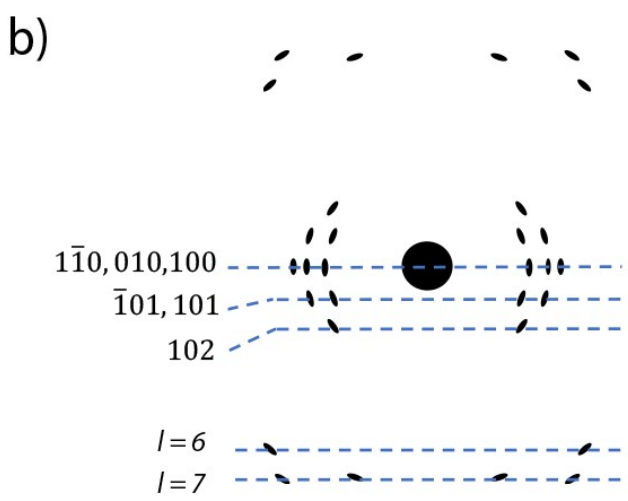

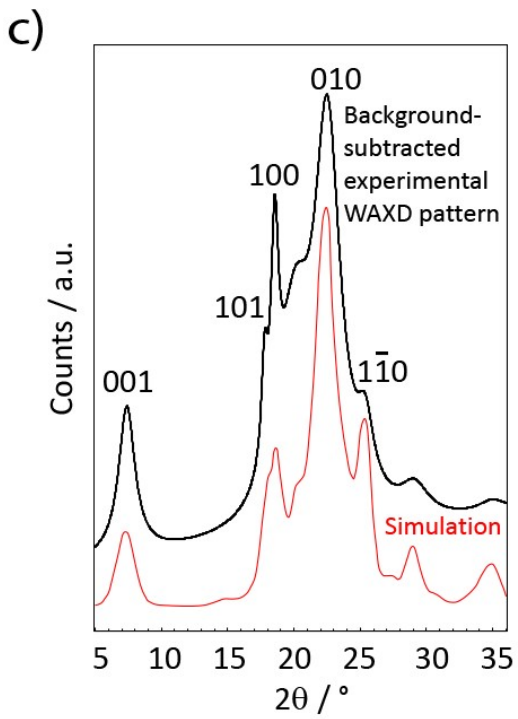

d)

d_{calc} [Å]	d_{exp} [Å]	$2\theta_{exp}$ [°]		Index
12.064	12.064	7.321	vs	001
6.032	6.039	14.67	w	002
4.995	4.989	17.78	s	101
4.778	4.784	18.55	vs	100
3.976	3.969	22.40	vs	010
3.525	3.526	25.26	w	1$\bar{1}$0
3.095	3.099	28.81	w	1$\bar{1}$1
2.569	2.564	35.00	w	116

Fig. S1 *a)* Electron fiber diffraction pattern from an oriented film of PA6TI (orientation direction vertical). *b)* Indexing of the electron fiber diffraction pattern according to a triclinic unit cell with lattice parameters a = 5.03 Å, b = 5.33 Å, c = 16.42 Å, a = 50.5 °, b = 79.0 °, g = 94.0 °. *c)* Indexed 1D-wide angle X-ray diffraction (WAXD) data from PA6TI compared with a simulated WAXD pattern (in red) corresponding to the model structure in Fig. 2a of the main text. *d)* Comparison of experimental d-spacings from WAXD and d-spacings calculated using the unit cell derived from the electron diffraction pattern in *b)*.

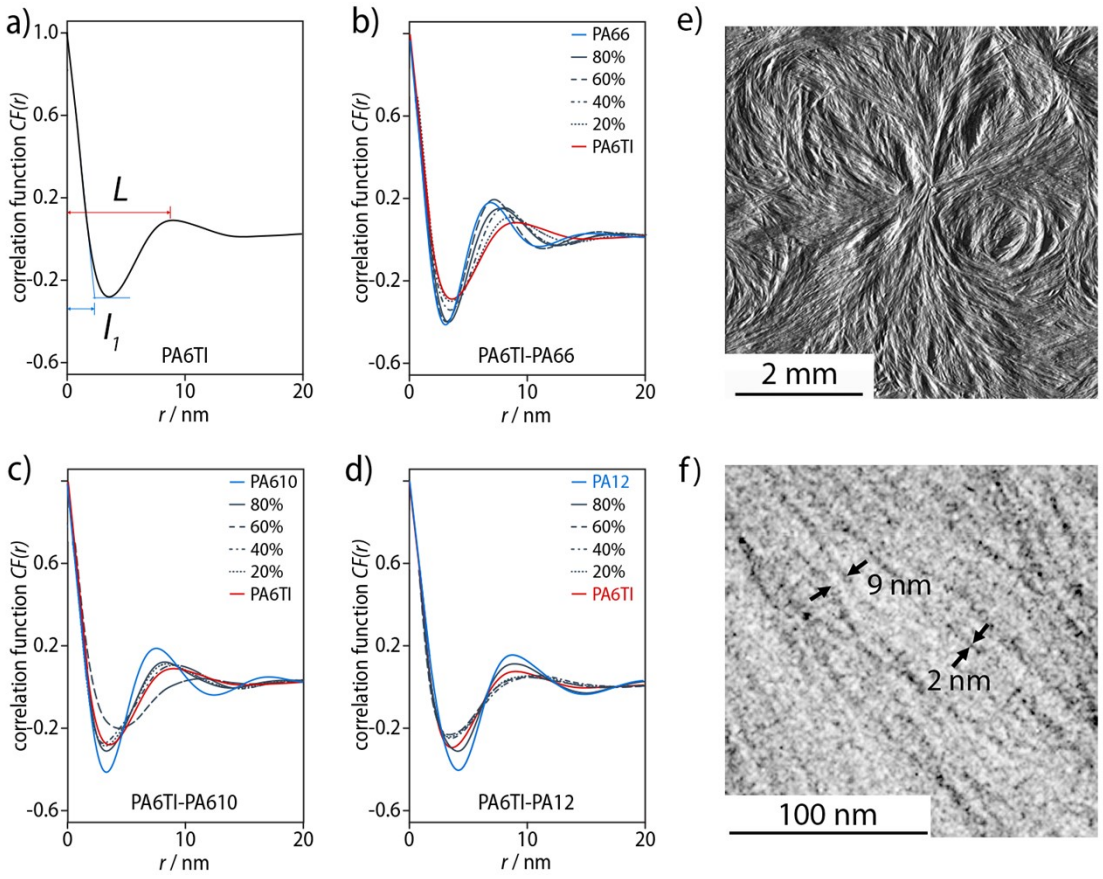

Fig. S2 *a)* 1D correlation function from small angle X-ray scattering (SAXS) data for PA6TI, illustrating the determination of the short spacing, l_1, from the first minimum and the long spacing, L, from the first maximum. [1,2] *b,c,d)* 1D correlation functions for melt-compounded PA6TI-PA66, PA6TI-PA610 and PA12 with various compositions. *e)* Intermittent-contact-mode atomic force microscopy (AFM) amplitude image (Bruker Nanoscope IIIa/MikroMasch NSC14 silicon probe) of a melt-crystallized PA6TI film showing the lamellar semicrystalline morphology characteristic of all the materials considered here. [3] *f)* Low-dose bright-field transmission electron micrograph (Thermo Scientific Talos™ F200S operated at 200 keV) from a 40 nm thick microtomed film of PA6TI recrystallized on a carbon substrate by cooling from 350 °C at 10 °C/min under nitrogen showing projections of individual lamella (dark regions) with minimum thicknesses of 2–3 nm and spacings of about 9 nm. l_1, which was about 2 nm for PA6TI, was therefore identified with the lamellar thickness, l, and L was identified with the mean lamellar long period. [1,2]

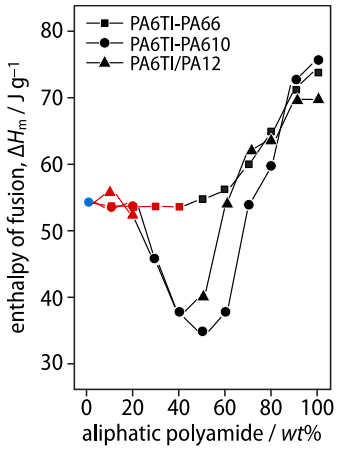

Fig. S3 Enthalpy of fusion, ΔH_m, determined by differential scanning calorimetry (DSC) for the copolyamides PA6TI-PA66 and PA6TI-PA610 as well as the blend PA6TI/PA12 as a function of composition. In materials containing up to 20 *wt*% of the aliphatic component, ΔH_m is insensitive to the nature of the aliphatic component and remains roughly constant (red). ΔH_m does not show a minimum in PA6TI-PA66 at intermediate compositions.

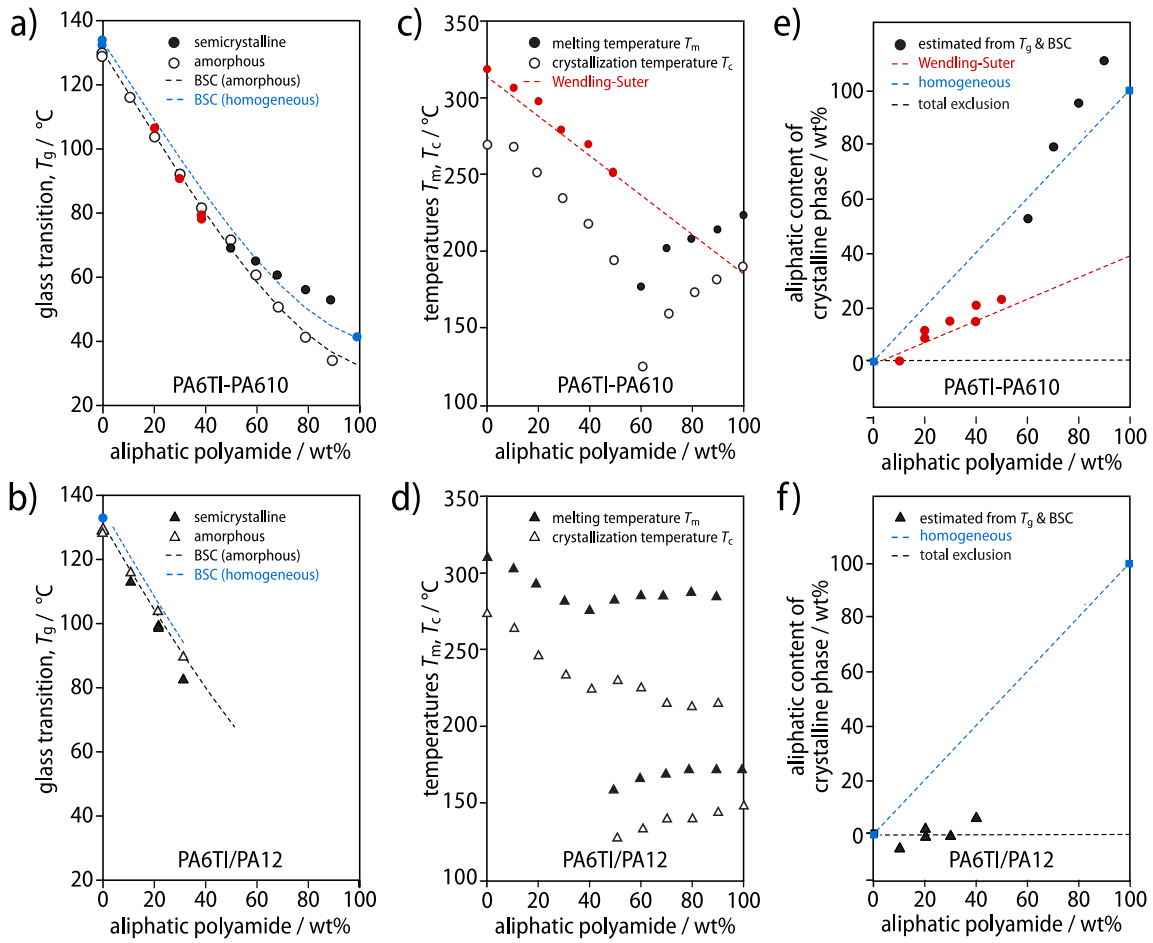

Fig. S4 *a,b)* Glass transition temperatures, T_g, corresponding to the mid-point of the calorimetric glass transition observed in DSC heating scans at 10 K/min on fully amorphous specimens of PA6TI-PA610 and PA6TI/PA12, respectively, obtained by quenching from the melt, and semicrystalline specimens obtained by cooling from 330 °C at 10 K/min. A fit to the data for the amorphous specimens (black curve) is obtained by adjusting the parameters k_1 and k_2 in the Brekner-Schneider-Cantow (BSC) expression for miscible binary blends of two components A and B.[4] The confining effect of the lamellae in semicrystalline specimens with a homogeneous distribution of the two components between the amorphous and the crystalline phase is modelled using the same values of k_1 and k_2, but with T_{gA} and T_{gB} shifted to match the experimental T_g obtained for semicrystalline PA6TI, PA610 or PA12 (dashed blue curve). Deviations between the model T_g and experimental T_g are then interpreted to reflect differences between the composition of the amorphous phase and the overall composition (Appendix A). *c,d)* Crystallization peak temperatures, T_c, as a function of composition for PA6TI-PA610 and PA6TI/PA12 cooled from 330 °C at 10 K/min and melting points, T_m, obtained from subsequent heating scans together with a fit of the Wendling-Suter expression to T_m for the random copolymer PA6TI-PA610 (Appendix B). *e,f)* Aliphatic content of the crystalline phase estimated from the T_g data in *a,b)* and the SAXS data in Fig. 3f, together with values implied by the Wendling-Suter expression used to fit the data in *c)* (red curve).

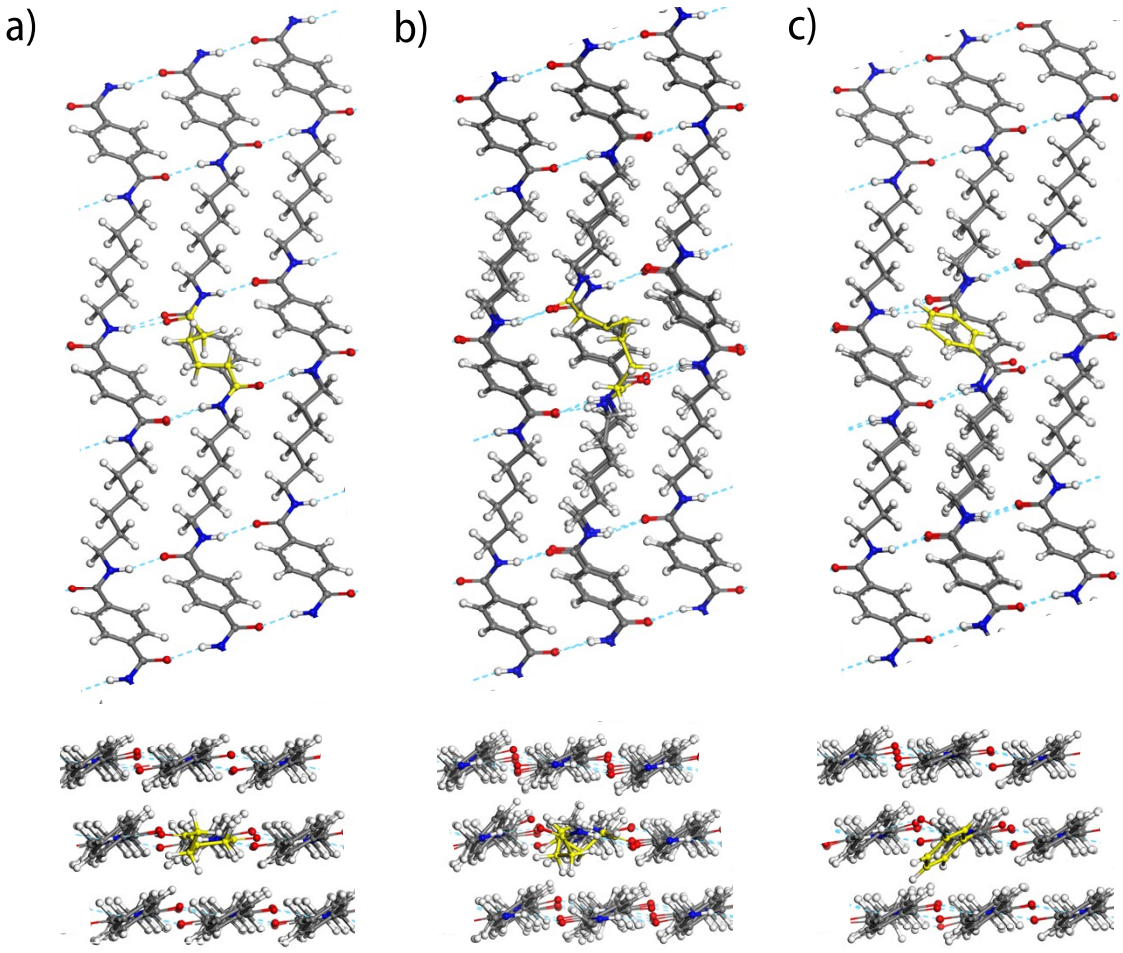

Fig. S5 Projections along (010) and (001) of relaxed PA6T crystalline structures in which a single terephthaloyl (T) unit has been replaced by *a)* an adipoyl unit, *b)* a sebacoyl unit, or *c)* an isophthaloyl (I) defect unit (highlighted in yellow). The displacement field induced by the defect is in each case associated with atomic displacements of the surrounding chains of less than 1 Å and is limited to chains adjacent to the defect, so that the long-range packing of the PA6T crystal remains unaffected. Introduction of a sebacoyl or an I unit disrupts hydrogen bonding, whereas introduction of an adipoyl unit maintains the original hydrogen bonding pattern of the T unit.

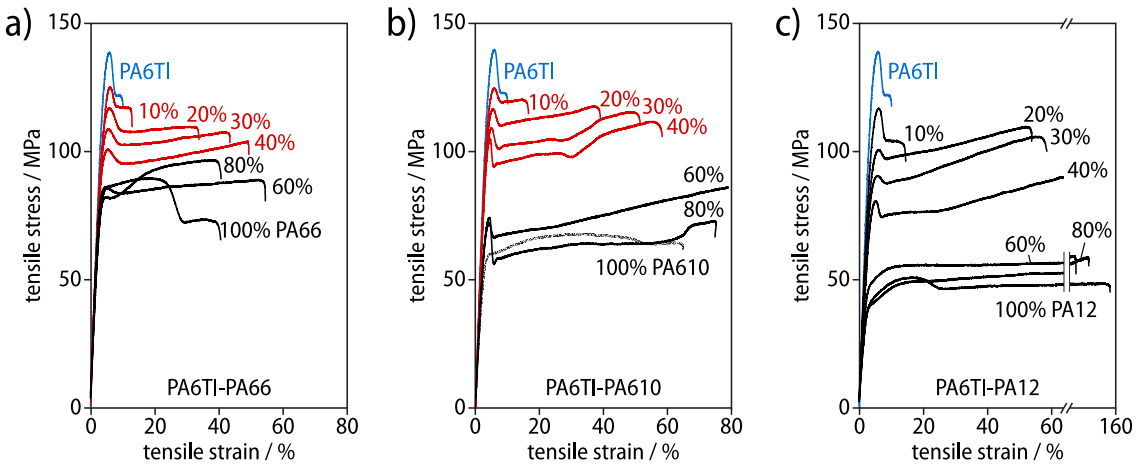

Fig. S6 *a-c)* Representative stress-strain curves from tensile tests at ambient temperature and 10 mm/min on dry injection moldings of melt compounded PA6TI-PA66, PA6TI-PA610, and PA6TI/PA12 for the aliphatic contents indicated (in *wt*%).

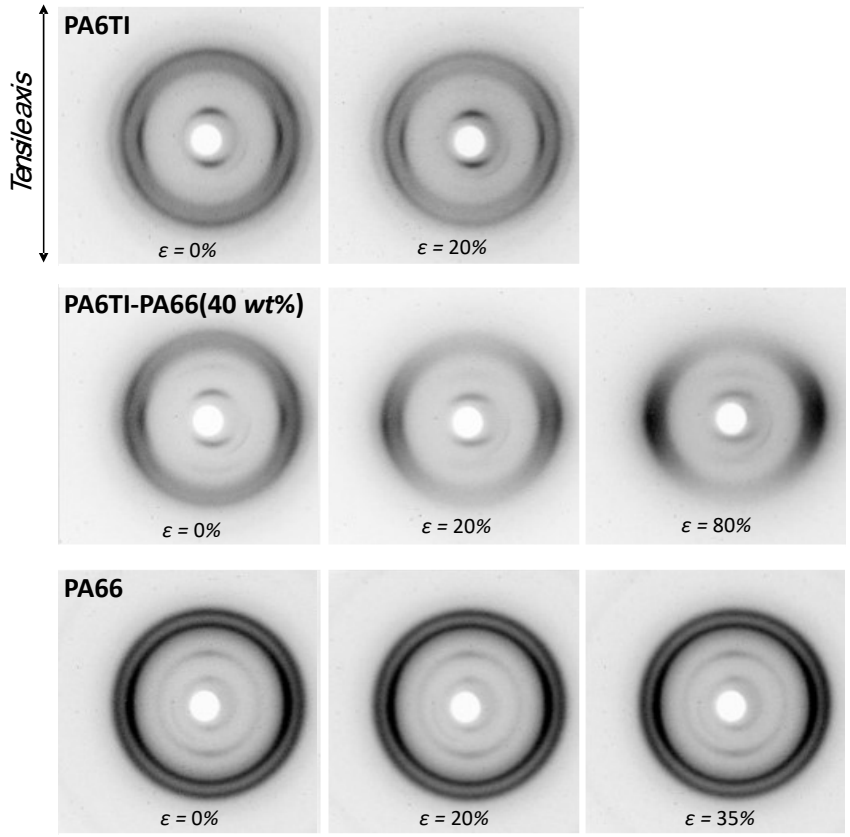

Fig. S7 2D-WAXD patterns from PA6TI, PA6TI-PA66(40 *wt*%), and PA66 obtained in transmission mode in the undeformed state and *in situ* at the nominal tensile strains indicated (specimen/tensile axis vertical). The diffuse asymmetric reflections at Bragg angles of about 10 ° in the bottom right-hand quadrant for PA6TI and PA6TI-PA66(40 *wt*%) and in the bottom left-hand quadrant for PA66 are artefacts due to diffusion from a Kapton window placed at the end of the X-ray tube.

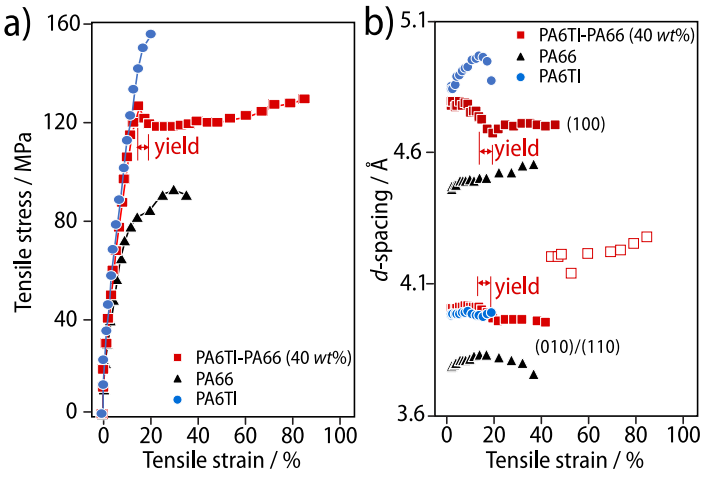

Fig. S8 *a)* Stress-strain behavior corresponding to the *in situ* WAXD experiments. The tensile stress is the average value of the stress measured during recording of the 2D-WAXD pattern (see the Experimental Part S3). *b)* The (100) and (010) spacings (the (110)/(010) spacings in the case of PA66) of PA6TI, PA6TI-PA66(40 *wt*%), and PA66 as a function of tensile strain.

Appendix A: Determination of the Composition of the Amorphous Phase from T_g Measurements

In amorphous specimens of the copolymers prepared by quenching from the melt, T_g shows a monotonic decrease with increasing aliphatic content that may be fitted using the Brekner-Schneider-Cantow expression (1) for miscible binary blends of two components A and B:[4]

$$T_g(\phi) = T_{gA} + (T_{gB} - T_{gA})\left[(1 + k_1)\phi - (k_1 + k_2)\phi^2 + k_2\phi^3\right] \quad \text{(A1)}$$

where ϕ is the mass fraction of component B, and k_1 and k_2 are empirical constants. After crystallization by cooling from 330 °C at 10 K/min, conditions that closely reproduce the melting behavior of the injection moldings, T_g increases in PA6TI and in the aliphatic homopolymers, presumably owing to confinement by the crystalline phase. The dashed red lines in Fig. 4a-c are obtained by interpolating the Brekner-Schneider-Cantow (BSC) expression using the same parameters k_1 and k_2 as for the fully amorphous specimens (the dashed red lines in Fig. 3a-c) but adjusting T_{gA} and T_{gB} to take into account the shifts associated with crystallization. We then assume deviations between the measured T_g in the semicrystalline specimens and the T_g values obtained by interpolation to reflect preferential segregation of the aliphatic units to either the amorphous or the crystalline phase. Expulsion of I units into the amorphous phase during crystallization of PA6TI was assumed to have a negligible influence on T_g given the comparable T_g of PA6TI and PA6I ($T_g \approx$ 124 °C for PA6I as opposed to $T_g \approx$ 130 °C for PA6TI). The local composition of the amorphous phase may hence be estimated directly from the measured T_g and the BSC expression, and the composition of the crystalline phase (Fig. 4d) may in turn be determined from the overall degree of crystallinity implied by Fig. 3f.

Appendix B. The Melting Point, T_m, as a Function of Comonomer Content

The equilibrium melting point of a polymer with infinite molar mass is given by

$$T_m^0 = \frac{\Delta H_m^0}{\Delta S_m^0} \quad \text{(A2)},$$

where $^{\Delta H_m^0}$ and $^{\Delta S_m^0}$ are the molar enthalpy of fusion and the molar entropy of fusion. $^{\Delta H_m^0}$ for PA6T may be estimated from $^{\Delta H_m}/\chi_w \approx 234\ J/g$ where $^{\Delta H_m}$ and χ_w are the observed enthalpy of fusion [J/g] and mass fraction of crystallinity in PA6TI, assuming the I units to be excluded from the crystalline phase (χ_w is estimated from the SAXS value for χ, assuming crystalline and amorphous densities of 1.25 g/cm^3 and 1.1 g/cm^3 for PA6TI). This leads to $^{\Delta H_m^0} \approx 56.4\ kJ/mol$, which is close to literature values of 56.5 kJ/mol for PA66, indicating the much higher melting point of PA6T (around 360 °C) than that of PA66 moldings (about 260 °C) to be primarily due to differences in chain stiffness, through their influence on $^{\Delta S_m^0}$. $^{T_m^0}$ is not well known for polyamides but is assumed to be about 40 K higher than ^{T_m} in the present case,[5] which leads to $^{\Delta S_{PA66}^0}$= 98.6 and $^{\Delta S_{PA6T}^0}$= 83.8 J/K/mol for PA66 and PA6T respectively. $^{\Delta S_m^0}$ is further assumed to be inversely proportional to the Kuhn length b so that $^{\Delta S_m^0(X)}$ in a hypothetical crystal containing a mole fraction X of PA66 units is

$$\Delta S_m^0(X) = \frac{\Delta S_{PA6T}^0}{1 - X + X\dfrac{\Delta S_{PA6T}^0}{\Delta S_{PA66}^0}} \quad \text{(A3)}.$$

If $^{\Delta H_m^0}$ is independent of X,

$$T_m^0(X) = \frac{\Delta H_m^0}{\Delta S_{PA6T}^0}\left(1 - X + X\frac{\Delta S_{PA6T}^0}{\Delta S_{PA66}^0}\right) \quad \text{(A4)}.$$

According to the approach of Wendling and Suter,[6] modified to include three types of comonomer, A, B and C, where B may coexist with A in the crystalline phase with an energy penalty ε, but C is entirely excluded:

$$\frac{1}{T_m^0(X)} - \frac{1}{T_m} = \frac{R}{\Delta H_m^0}\left\{ln\left(1 - X_B - X_c + X_B\, exp\left(-\frac{\varepsilon}{RT_c}\right)\right) - \langle\xi\rangle^{-1}\right\} \quad \text{(A5)},$$

where

$$\langle \xi \rangle^{-1} = 2\left(\left(X_B + X_c - X_B \, exp\left(-\frac{\varepsilon}{RT_c} \right)\right).\left(1 - \ X_B - X_c + X_B \, exp\left(-\frac{\varepsilon}{RT_c} \right)\right)\right) \quad \text{(A6)},$$

T_c is the crystallization temperature and R is the universal gas constant. For 70:30 PA6TI containing a mole fraction X_B of PA66 units, the proportion X_c of I units is given by

$$X_c = 0.3(1 - X_B) \quad \text{(A7)}$$

and $T_m^0(X)$ in Equation A5 is estimated by setting $X = X_B$ in Equation A4.

References

1. G. R. Strobl and M. Schneider, Direct evaluation of the electron density correlation function of partially crystalline polymers, *Journal of Polymer Science, Polymer Physics Edition,* 1980, **18**, 1343.

2. Z.-G. Wang, B. S. Hsiao, B. X. Fu, L. Liu, F. Yeh, B. B. Sauer, H. Chang, J. M. Schultz, Correct determination of crystal lamellar thickness in semicrystalline poly(ethylene terephthalate) by small-angle X-ray scattering, *Polymer*, 2000, **41**, 1791–1797.

3. J. Cretenoud, S. Galland, C. J. G. Plummer, V. Michaud, A. Bayer, N. Lamberts, B. Hoffmann and H. Frauenrath, High-temperature copolyamides obtained by the efficient transamidation of crystalline–crystalline polyamide blends, *Journal of Applied Polymer Science*, 2017, **134**, 44349.

4. M.-J. Brekner, H. A. Schneider and H.-J. Cantow, Approach to the composition dependence of the glass transition temperature of compatible polymer blends: 1, *Polymer*, 1988, **29**, 78–85.

5. J. H. Magill, M. Girolamo and A. Keller, Crystallization and morphology of nylon-6,6 crystals: 1. Solution crystallization and solution annealing behaviour, *Polymer*, 1982, **22**, 43–55.

6. J. Wendling and U. W. Suter, A New Model Describing the Cocrystallization Behavior of Random Copolymers, *Macromolecules*, 1998, **31**, 2516–2520.